THE JOURNAL OF BIOLOGICAL CHEMISTRY VOL. 283, NO. 9, pp. 5708–5718, February 29, 2008

A Temperature-sensitive Mutation in the *Arabidopsis thaliana* Phosphomannomutase Gene Disrupts Protein Glycosylation and Triggers Cell Death*

Received for publication, June 18, 2007, and in revised form, December 13, 2007 Published, JBC Papers in Press, December 17, 2007, DOI 10.1074/jbc.M704991200

Frank A. Hoeberichts[‡§1], Elke Vaeck[‡§1,2], Guy Kiddle[¶3], Emmy Coppens[‡§], Brigitte van de Cotte[‡§], Antoine Adamantidis[‖4], Sandra Ormenese[‖5], Christine H. Foyer[¶6], Marc Zabeau[‡§], Dirk Inzé[‡§], Claire Périlleux[‖], Frank Van Breusegem[‡§1,7], and Marnik Vuylsteke[‡§1]

From the [‡]Department of Plant Systems Biology, Flanders Institute for Biotechnology (VIB) and the [§]Department of Molecular Genetics, Ghent University, 9052 Gent, Belgium, [¶]Crop Performance and Improvement Division, Rothamsted Research, Harpenden AL5 2JQ, United Kingdom, and [‖]Department of Plant Physiology, University of Liège, 4000 Liège, Belgium

Eukaryotic phosphomannomutases (PMMs) catalyze the interconversion of mannose 6-phosphate to mannose 1-phosphate and are essential to the biosynthesis of GDP-mannose. As such, plant PMMs are involved in ascorbic acid (AsA) biosynthesis and *N*-glycosylation. We report on the conditional phenotype of the temperature-sensitive *Arabidopsis thaliana pmm-12* mutant. Mutant seedlings were phenotypically similar to wild type seedlings when grown at 16–18 °C but died within several days after transfer to 28 °C. This phenotype was observed throughout both vegetative and reproductive development. Protein extracts derived from *pmm-12* plants had lower PMM protein and enzyme activity levels. *In vitro* biochemical analysis of recombinant proteins showed that the mutant PMM protein was compromised in its catalytic efficiency (K_{cat}/K_m). Despite significantly decreased AsA levels in *pmm-12* plants, AsA deficiency could not account for the observed phenotype. Since, at restrictive temperature, total glycoprotein patterns were altered and glycosylation of protein-disulfide isomerase was perturbed, we propose that a deficiency in protein glycosylation is responsible for the observed cell death phenotype.

Phosphomannomutases (PMMs)[8] catalyze the interconversion of mannose 6-phosphate and mannose 1-phosphate and are required for the synthesis of GDP-mannose (Fig. 1). Both prokaryotes and eukaryotes utilize GDP-mannose in the synthesis of complex structural carbohydrates. Accordingly, this sugar nucleotide contributes to the synthesis of different structural carbohydrates in plant cell walls (1) and fulfills a key role in the biosynthesis of ascorbic acid (AsA) in plants (2, 3). GDP-mannose is also essential for post-translational modifications, such as protein glycosylation and glycosylphosphatidylinositol (GPI) anchoring in eukaryotes, because mannose, derived from GDP-mannose, is a crucial building block of the core glycan chain attached to the modified proteins (4, 5).

Because of their involvement in such fundamental processes, mutations in *PMM* genes often lead to severe and pleiotropic phenotypes. In the yeast *Saccharomyces cerevisiae*, a temperature-sensitive (ts) mutant affected in the *PMM* homolog *SEC53* is arrested in growth at restrictive temperature. In fact, *SEC53* has been classified as an essential gene because of the lethal phenotype of its null mutant (6, 7). Furthermore, *PMM* gene deletion mutants of the protozoan parasite *Leishmania mexicana* remain viable but are no longer able to establish an infection (8). In mouse, disruption of the *PMM2* gene causes early embryonic lethality (9), and in humans mutations in *PMM2* lie at the basis of Jaeken syndrome (also termed carbohydrate-deficient glycoprotein syndrome type Ia), a severe clinical disorder that provokes impaired neurological development and increased childhood mortality (10). In both *S. cerevisiae* and humans, defects in protein glycosylation due to lack of GDP-mannose have been pinpointed as the underlying cause for the observed phenotypes (7, 10).

The AsA deficiency of the *Arabidopsis thaliana vitamin c1* (*vtc1*) mutant demonstrated that GDP-mannose is also involved in the biosynthesis of AsA (11). The *VTC1* locus encodes a GDP-mannose pyrophosphorylase (GMPP), the enzyme that produces GDP-mannose from mannose 1-phos-

* This work was supported by Interuniversity Poles of Attraction Programme-Belgian Science Policy Grant P5/13, Research Fund of Ghent University Geconcerteerde Onderzoeksacties Grant 12051403, and Research Foundation-Flanders Grant G.0350.04. The costs of publication of this article were defrayed in part by the payment of page charges. This article must therefore be hereby marked "*advertisement*" in accordance with 18 U.S.C. Section 1734 solely to indicate this fact.

[1] These authors contributed equally to this work.
[2] Recipient of a predoctoral fellowship of the Institute for the Promotion of Innovation by Science and Technology in Flanders. Present address: Ablynx N.V., 9052 Gent, Belgium.
[3] Present address: Lumora Ltd., Ely CB7 4ET, United Kingdom.
[4] Present address: Dept. of Psychiatry and Behavioral Sciences, Stanford University, Palo Alto, CA 94304-5742.
[5] Present address: Dept. of Pathology, University Hospital of Liège, 4000 Liège, Belgium.
[6] Present address: School of Agriculture, Food and Rural Development, University of Newcastle upon Tyne, Newcastle upon Tyne NE1 7RU, United Kingdom.
[7] To whom correspondence should be addressed: Dept. of Plant Systems Biology, VIB, Ghent University, Technologiepark 927, 9052 Gent, Belgium. Tel.: 32-9-3313800; Fax: 32-9-3313809; E-mail: frank.vanbreusegem@psb.ugent.be.

[8] The abbreviations used are: PMM, phosphomannomutase; AFLP, amplified fragment length polymorphism; AsA, ascorbic acid; ConA, concanavalin A; EMS, ethyl methanesulfonate; GMPP, GDP-D-mannose pyrophosphorylase; GPI, glycosylphosphatidylinositol; InDel, insertion/deletion; MS, Murashige and Skoog; PDI, protein-disulfide isomerase; ts, temperature-sensitive; BC, back-crossed; Mb, megabase(s).

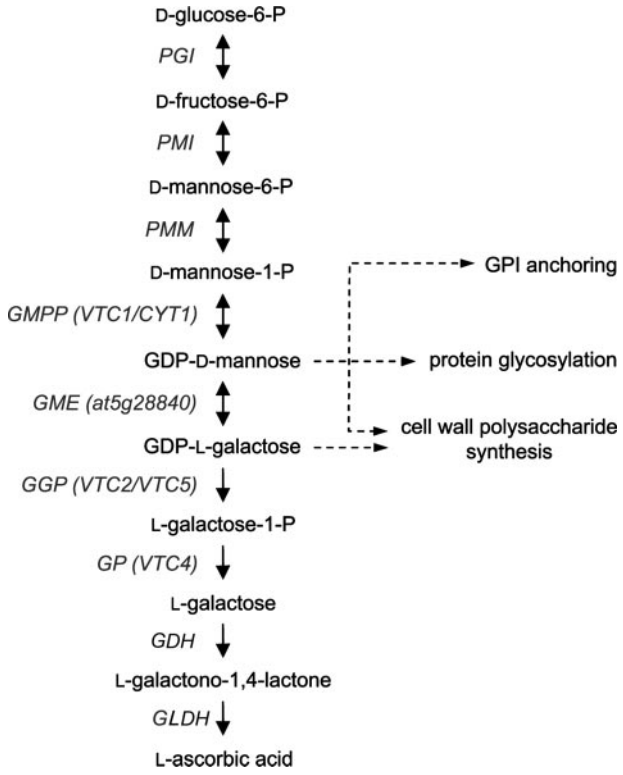

FIGURE 1. **PMM has diverse biological roles in higher plants.** PMM is required for the synthesis of GDP-mannose that is essential for AsA biosynthesis; posttranslational modifications, such as protein glycosylation and GPI anchoring; and the synthesis of different structural polysaccharides in the cell wall. *PGI*, phosphoglucose isomerase; *PMI*, phosphomannose isomerase; *GME*, GDP-D-mannose 3′,5′-epimerase; *GGP*, GDP-L-galactose phosphorylase; *GP*, L-galactose-1-P-phosphatase; *GDH*, L-galactose dehydrogenase; *GLDH*, L-galactono-1,4-lactone dehydrogenase.

phate and acts immediately downstream of PMM (Fig. 1). As a consequence, *vtc1* plants contain only ~25% of wild type AsA levels (11, 12). Very recently, evidence has been provided for the role of PMM in AsA biosynthesis in plants (3). Reduction of *PMM* expression levels through virus-induced gene silencing caused a substantial decrease in AsA content in *Nicotiana benthamiana* leaves, whereas raising *PMM* expression levels using viral vector-mediated ectopic expression resulted in an increase in AsA content. Consistently, overexpression of *PMM* in *Arabidopsis* also increased AsA content. However, no *Arabidopsis* T-DNA insertional knock-out mutants were reported, and attempts to produce knockdown plants using RNA interference technology were unsuccessful, suggesting that the *PMM* gene is essential. This inability to obtain plants with permanently decreased PMM levels impeded further studies into the possible involvement of PMM in other cellular processes (3).

Here, we screened an ethyl methanesulfonate (EMS)-mutagenized population of *Arabidopsis* seeds in search for ts mutations affecting plant growth and development. Screening for conditional mutants provides an unbiased means to identify essential genes. Contrary to null mutants generated via T-DNA insertional mutagenesis, conditional mutants generally allow for straightforward cultivation and propagation under specific (permissive) conditions. ts mutations are the most widely used type of conditional mutations and are usually characterized by a marked drop in activity of the gene product when the gene is expressed above (or below) a certain temperature. We describe the identification, positional cloning, and detailed characterization of a ts *Arabidopsis* mutant affected in the *PMM* gene. Upon exposure to restrictive temperature, *pmm-12* mutant plants were marked by reduced PMM enzyme activity and protein levels, developmental arrest, and subsequent cell death. The *pmm-12* mutant plants also had a lower AsA content, but it is demonstrated that this AsA deficit cannot account for the cell death phenotype. Instead, we propose that a ts deficiency in protein glycosylation is responsible for the observed cell death phenotype.

EXPERIMENTAL PROCEDURES

Plant Material, Growth Conditions, and Screening Procedure—*A. thaliana* (L.) Heyhn. (ecotype Col-0) plants were grown either on Murashige and Skoog (MS) medium, including 10 g/liter sucrose or in soil at continuous light (~60 μmol of photons m^{-2} s^{-1}), unless otherwise stated. The permissive temperature used was either 16 or 18 °C, and the restrictive temperature was 28 °C.

The *pmm-12* line was generated by treating ~200,000 seeds with 15 μM EMS for 24 h at 24 °C. Mutagenized seeds (M_1) were subdivided into batches consisting of ~1000 individual seeds (25 mg), grown at 18 °C, and allowed to self-pollinate, resulting in the corresponding M_2 seed batches. For 150 M_2 batches, aliquots of 25 mg of seeds were plated, grown at permissive temperature for 7 days, and subsequently screened for ts growth defects at restrictive temperature. Seedlings grown on MS medium containing 1 μM 1-naphthaleneacetic acid that showed growth defects within 4 days after transfer to restrictive temperature (compared with wild type) were considered putative mutants and subsequently rescued by transferring them back to the permissive temperature on fresh MS medium. Heritability of the observed phenotype was tested with M_3 plants produced by self-fertilization of M_2 plants of putative mutants. M_3 seeds were used to characterize the identified mutants.

For complementation, the *AtPMM* cDNA was first cloned into pDONR221 and subsequently cloned into the binary vector pK7WG2D (13) using Gateway technology (Invitrogen). M_3 plants were transformed at permissive temperature via the floral dip method (14).

DNA Extraction—Individual plants were ground and mixed with 400 μl of buffer composed of 200 mM Tris-HCl (pH 7.5), 2 M NaCl, 50 mM EDTA, and 2% *N*-cetyl-*N*,*N*,*N*-trimethylammonium bromide, followed by a 60-min incubation at 65 °C. After 15 min on ice, samples were extracted once with 250 μl of chloroform/isoamylalcohol (24:1). The aqueous phase was mixed with 200 μl of isopropyl alcohol, and samples were centrifuged. The DNA pellet was rinsed once with 70% ethanol, air-dried, and resuspended in 50 μl of 1 mM Tris-HCl (pH 8.0) and 0.1 mM EDTA.

Map-based Cloning and Fine Mapping—To obtain *pmm-12* mutants with a more homogeneous genetic background, *pmm-12* M_3 mutants were back-crossed (BC) into the Col-0 wild type genetic background. The resulting BC_1 plants were self-fertilized to obtain BC_1F_2 seeds, and the 3:1 (wild type/mutant) segregation ratio was tested at restrictive temperature.

Subsequently, mutant BC_1F_2 plants were rescued by transfer to soil and growth at the permissive temperature. Self-pollination of these mutant plants led to lines whose genetic background was purified by 50%. Homogeneity of the resulting BC M_3 mutant lines was verified by growing at least 50 plants and checking the consistency of the mutant phenotype at restrictive temperature. To generate mapping populations, BC M_3 mutant lines were reciprocally crossed with Landsberg *erecta* (L*er*) wild type.

In a first step, a genome-wide mapping procedure using the physical AFLP map described by Peters *et al.* (15, 16), was applied to 310 F_2 plants to determine the chromosomal location of the *PMM* gene. All AFLP markers, including the 85 Col-0/L*er* framework AFLP markers resulting from a standard set of AFLP SacI/MseI primer combinations, were generated as described (17). AFLP markers were scored co-dominantly with the aid of the specific image analysis software AFLP-QuantarPro (Keygene Products, Wageningen, The Netherlands). For fine-mapping, a large population of 9,900 F_2 segregants were phenotyped, and 1,317 F_2 mutants (13.3%) were selected for further fine mapping of the mutant locus. In the case of a monogenic recessive trait, F_2 mutants are the individuals of choice. These 1,317 mutant F_2 segregants were subsequently genotyped for insertion/deletion (InDel) polymorphisms of the Cereon InDel collection (18). In the subsequent steps, gradually decreasing subsets of recombinants were genotyped with pairs of InDel markers flanking the genomic area containing the *PMM* gene until no recombinants were left. InDel polymorphisms were scored co-dominantly. PCR primers were designed based on the *Arabidopsis* genome sequence (available on the World Wide Web) using Primer3 software (19). The conditions used for PCR amplification were as follows: 2 min at 94 °C; 10 cycles of 15 s at 94 °C, 30 s at 63 °C, 30 s at 72 °C with a touch-down of 1 °C per cycle; 35 cycles of 15 s at 94 °C, 30 s at 53 °C, 30 s at 72 °C; 2 min at 72 °C.

Sequence Analysis—PCR primers were designed based on the *Arabidopsis* information resource (TAIR) annotation (available on the World Wide Web) using Primer3 software (19) to amplify 500-bp exonic and intronic fragments having a minimal overlap of 100 bp. Amplicons were amplified by PCR using 50 ng of genomic DNA template, Silverstar DNA polymerase (Eurogentec, Seraing, Belgium), and a final concentration of 0.5 μM for each primer. The conditions used for the PCR amplification were as follows: 2 min at 95 °C; 35 cycles of 30 s at 95 °C, 30 s at T_m (depending on the primer sets), 2 min at 72 °C. PCR products were purified with ExoSAP-IT (U.S. Biochemical Corp., Cleveland, Ohio) and transferred to a 96-well PCR plate (~10 ng/100 bp) together with 50 μM primer. After the plate had been dried at 65 °C for 30–120 min, sequencing mix and buffer were added. The conditions for a second PCR were as follows: 2 min at 95 °C; 40 cycles of 10 s at 95 °C, 10 s at 48 °C, 2 min at 60 °C. Samples were sequenced with an automated sequencer (ABI3700 or ABI377; Applied Biosystems Inc., Foster City, CA).

Production of Recombinant Proteins—The open reading frame of *PMM* (at2g45790) and its mutant isoforms were PCR-amplified using cDNA obtained from wild type or mutant plants as a template. The *pmm-1* mutation was introduced using the ATGGCGGCGAAAATTCCCAG primer, the *pmm-2* mutation with cDNA from *pmm-12* plants, and the above primer adapted to the wild type sequence. Fragments were cloned into pDONR221, verified by DNA sequence analysis, and then cloned into pDEST17 using Gateway technology (Invitrogen). *Escherichia coli* (strain BL21(DE3)pLysE) harboring the various constructs were, by means of a preculture, inoculated at OD 0.15 in 5 ml of Luria broth medium containing 100 μg/ml ampicillin and 25 μg/ml chloramphenicol. Cultures were subsequently grown for 1.5 h at 37 °C and induced with 0.2 mM isopropyl 1-thio-β-D-galactopyranoside. After 5 h of incubation at room temperature, 1 ml of bacteria was harvested. Recombinant proteins were purified with TALON metal affinity resin (Clontech), using 50 mM Hepes (pH 7.5), 300 mM NaCl, 10% glycerol, 1 mM phenylmethylsulfonyl fluoride (1:1.5, w/v) as equilibration buffer and equilibration buffer including 250 mM imidazole as elution buffer. Protein concentrations were determined according to Bradford (20).

Enzyme Activity Assays—PMM activity was determined via a coupled assay; the conversion of mannose 1-phosphate to mannose 6-phosphate was coupled to the reduction of $NADP^+$ to NADPH (catalyzed by glucose 6-phosphate dehydrogenase) through the activities of phosphomannose isomerase and glucose-6-phosphate isomerase. The reaction was monitored through the increase in absorbance at 340 nm as a result of the increase in NADPH. *In planta* PMM activity was determined essentially as described (21). In short, leaf tissue ground in liquid nitrogen was resuspended in 50 mM Hepes (pH 7.6), 10 mM $MgCl_2$, 5 mM dithiothreitol, 1 mM EDTA, 1 mM ethylene glycol-bis(β-aminoethyl ether) *N*,*N*,*N*′,*N*′-tetraacetic acid, 1 mM benzamidine hydrochloride, and 0.5 mM phenylmethylsulfonyl fluoride (1:1.5, w/v). Cell debris was removed by centrifugation, and sample supernatants were desalted on Sepharose G25 NAP5 columns (GE Healthcare). PMM activity was determined in a reaction mixture consisting of protein extract, 50 mM Hepes (pH 7.6), 10 mM $MgCl_2$, 0.1% bovine serum albumin, 1 mM NADP, 50 μM glucose 1,6-biphosphate (as a hexose biphosphate activator), 0.5 units/ml glucose-6-phosphate dehydrogenase, 0.5 units/ml phosphoglucose isomerase, and 0.5 units/ml phosphomannose isomerase. The reaction was initiated by the addition of the relevant concentration of D-mannose 1-phosphate, and the absorbance at 340 nm was recorded for 120 min. For each sample, material from at least 40 seedlings was pooled. *In vitro* activity of purified recombinant PMM was measured similarly in the same reaction mixture. The PMM content of each recombinant protein fraction was verified by protein gel blot analysis using penta-His antibody (Qiagen, Hilden, Germany).

Ascorbate Measurements and Protein Gel Blotting—The AsA content of control and mutant *Arabidopsis* leaves was determined as described previously (22, 23).

For concanavalin A (ConA) staining, 5 μg of total soluble (NAP5 column-purified) protein from *Arabidopsis* leaves was resolved on a 12.5% SDS-polyacrylamide gel and blotted onto a Hybond ECL membrane (GE Healthcare). The membrane was incubated for 1 h in PBSCT buffer (138 mM NaCl, 2.7 mM KCl, 10 mM Na_2HPO_4, 1.8 mM KH_2PO_4, 1 mM $MgCl_2$, 1 mM $CaCl_2$, 0.5% Tween 20, pH 7.2) and then for 1 h in PBSCT buffer con-

taining 0.1 mg/liter ConA conjugated to horseradish peroxidase (Sigma). The membrane was washed five times for 5 min with PBSCT. ConA-binding glycoproteins were detected with Western Lightning chemiluminescence reagent (PerkinElmer Life Sciences).

Wild type and *pmm-12* protein extracts for Western blotting were prepared as described (24). Protein extracts were separated on an 8% SDS-polyacrylamide gel and transferred onto a polyvinylidene fluoride membrane (Immobilon-P, Millipore, Billerica, MA). Rabbit antiserum against *Arabidopsis* PMM was raised using purified recombinant protein as the antigen (Eurogentec). The AtPMM antibody was used at a dilution of 1:2,500, and antibodies against *Arabidopsis* protein-disulfide isomerase (PDI) and SKU5 were used at a dilution of 1:2,500 and 1:1,000, respectively. Reacting material was visualized with goat anti-rabbit IgG secondary antibody conjugated to horseradish peroxidase (GE Healthcare), followed by a luminescence reaction (PerkinElmer Life Sciences). For each sample, material from at least 40 seedlings was pooled.

RESULTS

Identification of a ts Cell Death Mutant—An EMS-mutagenized population of ~200,000 *Arabidopsis thaliana* (ecotype Col-0) seeds was screened for deficiencies in growth and development when grown at a restrictive temperature of 28 °C. Candidate mutants with severe growth-related phenotypes were rescued by transfer to permissive temperature (16 to 18 °C) to allow self-pollination. M_3 progenies were rescreened to confirm the heritability of the ts phenotype, resulting in the isolation of 12 ts lines. General phenotypic analysis allowed classification of the 12 mutants into two categories; one category consisted of four mutants, specifically impaired in the formation of particular plant organs, and the other consisted of eight mutants that were inhibited in overall plant growth. The observed phenotype was either reversible or irreversible, which, at restrictive temperature, resulted in growth arrest or lethality, respectively (25). One of the identified mutants, initially designated *defective in growth 1* (*dgr1*), showed a growth arrest followed by cell death at restrictive temperature. After back-crossing *dgr1* M_3 plants to Col-0 wild type plants, a segregation analysis of the BC_1F_2 families revealed the recessive nature of the mutation (data not shown).

Map-based Cloning of the Mutant Locus—F_2 mapping populations were obtained by reciprocal crosses of BC *dgr1* mutant plants (Col-0) with L*er* wild type plants. Each F_1 cross was checked for heterozygosity with the SSLP marker "nga8" that is polymorphic between Col-0 and L*er* (26). Segregating F_2 populations were used for the subsequent map-based cloning process.

In a first step of the genome-wide mapping of *dgr1*, a total of 126 F_2 plants, together with the BC *dgr1* mutant plants (Col-0) and L*er* as parental lines, were analyzed with an initial set of eight primer combinations (15). Segregation analysis of the 85 AFLP markers revealed complete linkage of the mutant phenotype to a 4.7-Mb region on chromosome II bordered by the upper flanking marker SM240_448.2 and the lower end of chromosome II. In the next step, 13 additional primer combinations, amplifying AFLP markers in the vicinity and within the defined region of interest, were used for further linkage analysis. This way, the region containing the mutant locus could be narrowed down to 1.3 Mb, delimited by SM26_495.4 and the lower end of chromosome II. Because analysis of eight additional AFLP markers did not result in the identification of further recombinants for the 1.3-Mb region, an additional population of 184 F_2 plants was analyzed with other SacI/MseI AFLP markers polymorphic between Col-0 and L*er*, localized within the defined 1.3-Mb interval. This step allowed mapping of the affected gene to a 673-kb region delineated by the upper flanking marker SM120_153.8 and the lower flanking marker SM190_142.6. AFLP markers SM61_107.7 and SM117_193.1, localized within the 673-kb region (Fig. 2), showed complete linkage to the mutant phenotype.

For fine mapping of the mutant locus, an F_2 population of 9,900 plants was grown. Since the *DGR1* gene harbored a recessive mutation, homozygous and heterozygous wild type plants could not be distinguished solely based on their phenotypes. Therefore, to avoid the time-consuming step of self-fertilizing the relevant wild type recombinants and growing the F_3 progeny to determine their genotype, we only used the mutant F_2 individuals for subsequent analysis. In total, 1,317 F_2 mutants (13.3%) were identified, harvested, and submitted to linkage analyses using InDel markers developed from the Cereon InDel collection (18). Initially, two InDel polymorphisms (CER452389 and CER449256) flanking the previously defined 673-kb interval were identified and used to screen the F_2 mutant population. Forty recombinants were isolated and subsequently analyzed with six additional InDel markers localized in the region delineated by the two originally flanking InDel markers. As a result, the interval could be narrowed down to 224 kb with CER452385 and CER452346 as the upper and the lower flanking marker, respectively. The remaining nine recombinants were screened with 11 additional InDel markers localized within the 224-kb interval, finally resulting in a 35-kb region delimited by CER449813 and CER452353/54 that contained the *DGR1* gene (Fig. 2).

According to the gene annotations for chromosome II in the *Arabidopsis* genome data base (available on the World Wide Web), the 35-kb region comprising the *DGR1* gene encompassed 12 (putative) genes. To determine which of them carried the *dgr1* mutation, the 35-kb region was sequenced both in the mutant and wild type background. In mutant plants, we detected two differences (G19A and G101A) in gene at2g45790, relative to the sequence of the bacterial artificial chromosome clone F4I18. In the remaining 11 genes, no differences were detected. To verify the presence of the two mutations, the at2g45790 gene was sequenced in 20 Col-0 plants and in the 40 mutant recombinants that had been identified and used during the fine mapping of *dgr1*. Both mutations were absent from the wild type gene and present in all 40 mutant recombinants (data not shown).

The Mutant Locus Encodes a PMM—The at2g45790 gene that contained the two point mutations encoded a eukaryotic PMM. In the *Arabidopsis* genome, only one *PMM* gene is present (3). Therefore, we will hereafter refer to the *dgr1* mutant as the *pmm-12* mutant. The two point mutations, designated *pmm-1* and *pmm-2*, both occurred in the first exon. Compari-

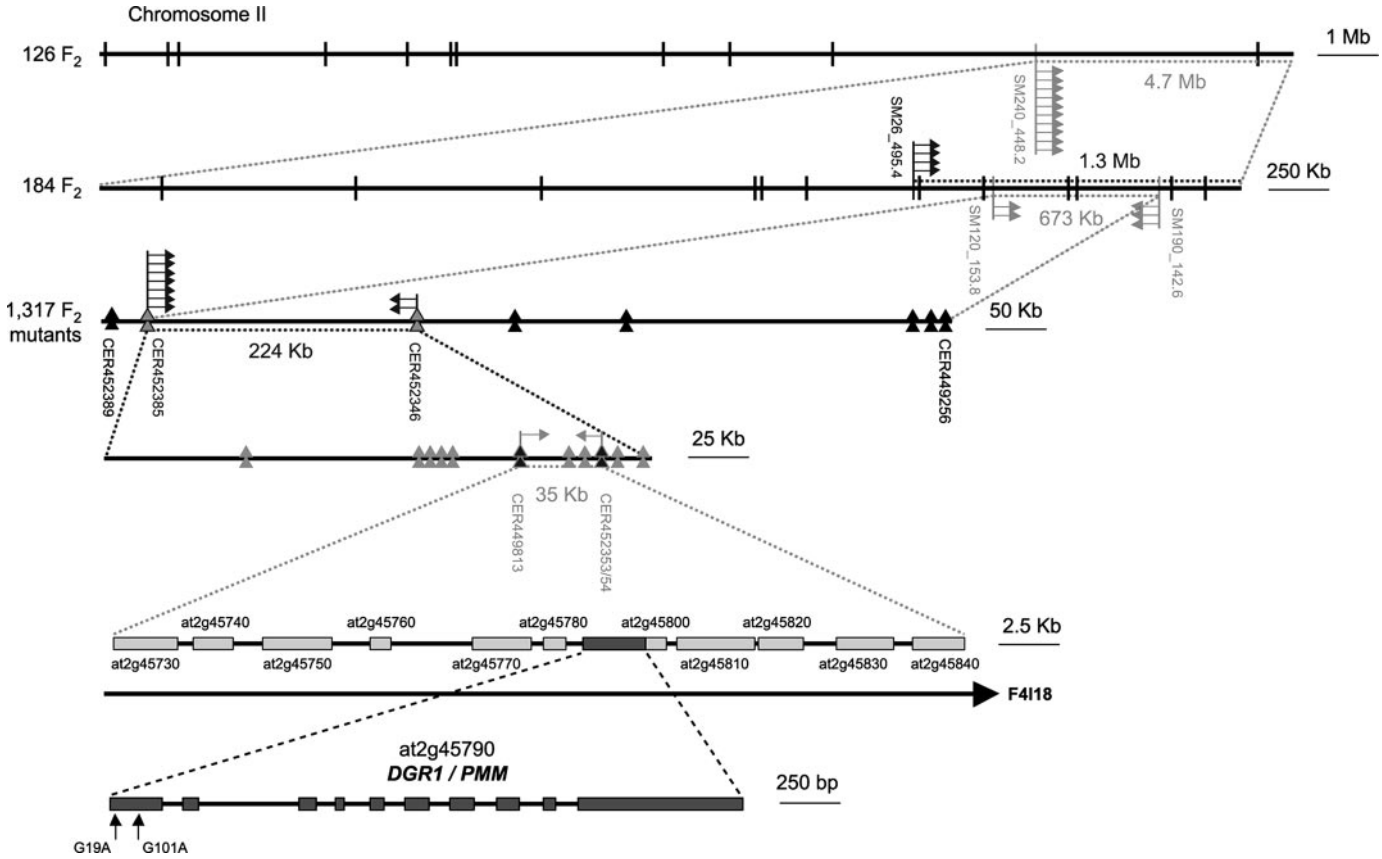

FIGURE 2. **Identification of the *DGR1*/*PMM* gene via map-based cloning.** A standard set of eight AFLP primers was applied to 126 F_2 individuals and identified a 4.7-Mb area at the bottom of chromosome II. Additional mapping with AFLP markers (*vertical bars*) on 184 F_2 individuals delineated the *DGR1/PMM* locus to 673 kb. AFLP markers are identified by the SM code referring to the corresponding SacI/MseI enzyme combination, followed by the code referring to the primer combination used and the estimated molecular size of the DNA fragment. Subsequently, 1,317 F_2 mutant individuals were screened with flanking InDel markers (*stacked triangles*; CER452389 and CER449256) and 40 recombinants (not shown) were used for fine mapping by means of InDels that defined the locus to 35 kb flanked by markers CER449813 and CER452353/54. The *arrows* mark recombinants relevant for further delineation of the region of interest. The 35-kb region contained 12 genes and was spanned by the bacterial artificial chromosome clone F4I18. Two point mutations were identified in gene at2g45790 that encodes a PMM. The gene structure of *PMM* is outlined with exons as *boxes*, and the two nucleotide changes are indicated.

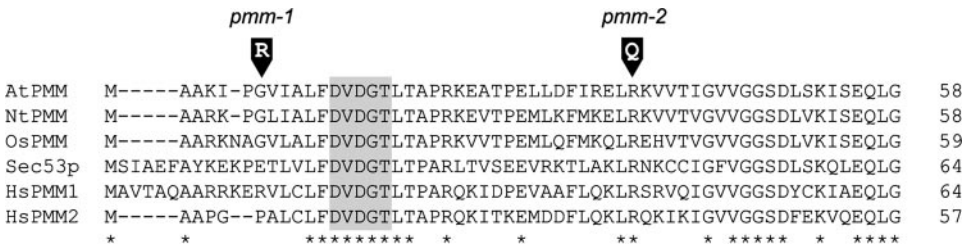

FIGURE 3. **Multiple alignment of part of the amino acid sequences of PMM proteins from *Arabidopsis* (*AtPMM*), tobacco (*NtPMM*), rice (*OsPMM*), budding yeast (*Sec53p*), and humans (*HsPMM1* and *HsPMM2*).** The *asterisks* indicate conserved amino acids. The *shaded region* marks the conserved amino-terminal DVDGT motif. Both nucleic acid replacements in the mutant (*pmm-1* and *pmm-2*) are indicated.

son of wild type and mutant cDNAs and their deduced amino acid sequences revealed that point mutation *pmm-1* resulted in a GGA to AGA codon change (codon 7), leading to a substitution of a neutral glycine residue with a basic arginine. The *pmm-2* mutation resulted in a CGA to CAA codon change (codon 37), thereby replacing an arginine with a neutral glutamine (Fig. 3). PMMs are phosphotransferases belonging to the superfamily of haloalkanoic acid dehalogenases (27). Members of the phosphotransferase branch share a conserved N-terminal D*X*D*X*(T/V) domain that is directly involved in the phosphoryl transfer (28). Both mutations were located outside this D*X*D*X*(T/V) motif. However, the *pmm-2* mutation affected a highly conserved arginine residue, whereas the *pmm-1* mutation involved the substitution of an apparently less conserved amino acid (Fig. 3).

Complementation and Identification of a T-DNA Insertional Mutant—To confirm that the mutations in the at2g45790 locus were responsible for the *pmm-12* phenotype, homozygous *pmm-12* plants were transformed with a construct containing the wild type at2g45790 coding region under control of the CaMV 35 S promoter. T_2 seeds with a 3:1 segregation ratio on selective medium, indicative of a single insertion locus, also unambiguously displayed a 3:1 phenotypic segregation ratio when grown on nonselective medium at restrictive temperature (data not shown). This indicated that the *pmm-12* mutant phenotype could be complemented by overexpression of the at2g45790 locus.

We retrieved the T-DNA insertion line 045D04 from the GABI-Kat collection (29). This line contains an insertion 5 bp

upstream from the start codon of the *PMM* gene, as verified via the standard GABI-Kat quality control on DNA extracted from T_2 seedlings (29). Unfortunately, none of the T_2 plants grown from the received seeds gave T_3 seeds that were 100% resistant to sulfadiazine. In other words, no transgenic lines homozygous for antibiotic resistance could be recovered. A closer look at T_3 plants revealed that the siliques of plants resistant to sulfadiazine lacked ~25% of the seeds, whereas siliques of nonresistant T_3 plants were undistinguishable from wild type siliques (data not shown), strongly suggesting that a knock-out mutation in at2g45790 causes embryo lethality.

The pmm-12 Mutant Has a ts Cell Death Phenotype—When grown *in vitro* at permissive temperature, 2-week-old *pmm-12* mutant seedlings did not show any obvious phenotype when compared with wild type Col-0 seedlings. However, when transferred to 28 °C, growth was inhibited, and seedlings died within several days (Fig. 4*A*). The first signs of cell death visible to the naked eye consisted of tissue browning at the base of developing leaves and in the shoot meristem (Fig. 4*B*) and became apparent after 4 days at 28 °C. In 6-week-old plants grown in soil at 16 °C under a 10-h photoperiod, cell death became visible only after exposure to 28 °C for at least 2 weeks (Fig. 4*C*). In addition, mutant *pmm-12* plants were germinated and grown in soil at 16 °C under continuous light conditions until flowering. These plants also displayed strong growth inhibition and completely wilted within 2 weeks after transfer to 28 °C (Fig. 4*D*).

Growth analysis of the primary root of germinating seedlings disclosed that, at permissive temperature, the growth rate of *pmm-12* roots was slightly decreased compared with that of wild type roots (Fig. 5*A*). Upon transfer to restrictive temperature, 7 days after germination, root growth rates of wild type plants significantly increased until plants were transferred back to 18 °C, 4 days later. In contrast, root growth of 7-day-old *pmm-12* seedlings was rapidly inhibited upon transfer to 28 °C. Root growth was completely arrested within 2 days and could not be rescued by placing the seedlings back to 18 °C after 4 days at 28 °C (Fig. 5, *B* and *C*). When root explants were transferred to callus-inducing medium and placed at 28 °C, *pmm-12* explants, in contrast to wild type explants, could not induce callus formation (data not shown). Taken together, we demonstrated that the ts cell death phenotype is conferred throughout both vegetative and reproductive development and that the progression of cell death depends on the plant's developmental stage.

pmm-12 Plants Exhibit Decreased PMM Enzyme Activity and Protein Levels—To determine the effect of the *pmm-12* mutation on PMM activity *in planta*, total PMM activity was monitored in extracts from wild type and *pmm-12* plants. Plants were first grown for 2 weeks at 16 °C and then transferred to 28 °C or kept at 16 °C. Shoot tissue was harvested 0 h, 24 h, 48 h, and 4 days after transfer, and PMM activity was monitored via a coupled assay. When grown at 16 °C, *pmm-12* plants had PMM activity significantly lower than that of wild type plants. At the beginning of the experiment (0 h), the conversion velocity (*V*) measured in *pmm-12* extracts was ~30% of that in wild type samples. After transfer to 28 °C, wild type plants showed a decrease in activity of ~25%, whereas activity in the mutant plants remained relatively stable (Fig. 6*A*).

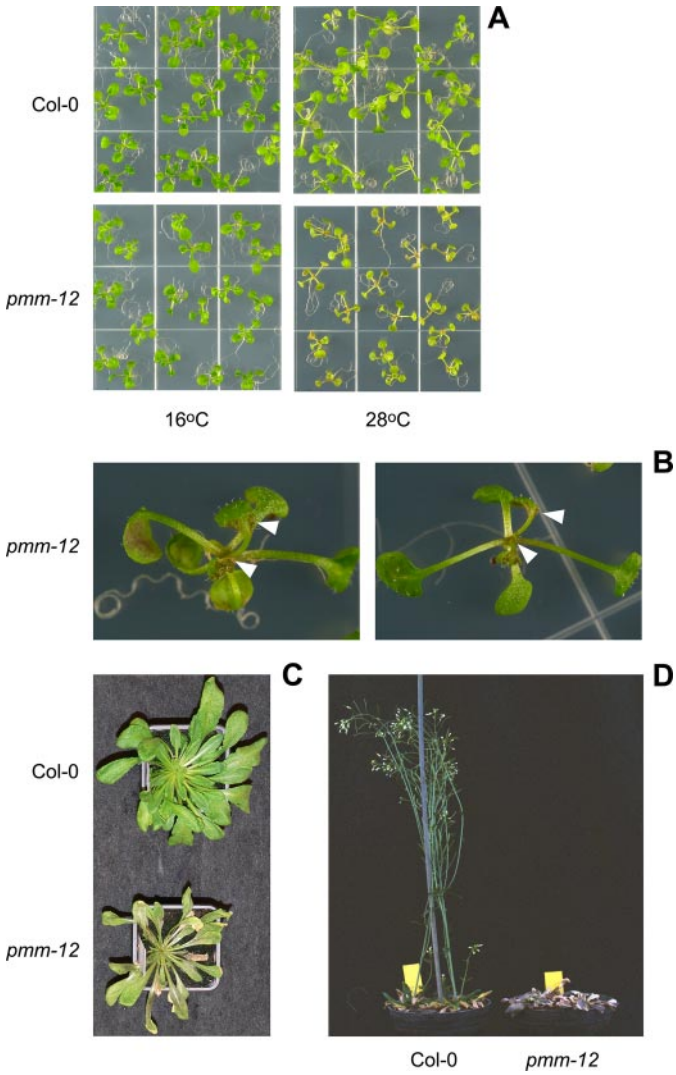

FIGURE 4. **Effects of transfer to 28 °C on the *Arabidopsis pmm-12* mutant.** *A*, mutant plants, grown for 2 weeks at 16 °C, appeared essentially identical to wild type Col-0 plants. Five days after transfer to 28 °C, mutant seedlings displayed growth arrest and severe browning of shoot tissue. *B*, the first signs of cell death became visible after 4 days at 28 °C at the base of developing leaves and in the shoot meristem (*arrows*). *C*, wild type and mutant plants germinated and grown in soil for 6 weeks at 16 °C under a 10-h photoperiod, 2 weeks after transfer to 28 °C. *D*, wild type and mutant plants germinated and grown in soil at 16 °C under continuous light conditions until the first flower buds appeared. The picture was taken 2 weeks after transfer to 28 °C.

Western blotting using a polyclonal AtPMM antibody revealed that *pmm-12* plants had considerably decreased PMM protein levels, both at 16 and 28 °C. Furthermore, the temperature shift to 28 °C had a negative effect on protein levels in wild type and in mutant plants (Fig. 6*B*). We conclude that *pmm-12* plants suffer from a considerable reduction in both total PMM activity and PMM protein levels.

The Different Mutant PMM Isoforms Have Altered Kinetic Properties—We assessed the impact of each of the identified point mutations on recombinant enzyme activity. Consequently, four different *Arabidopsis* PMM isoforms were tested: the wild type enzyme, two isoforms containing one of the identified mutations each (PMM-1 and PMM-2), and one isoform

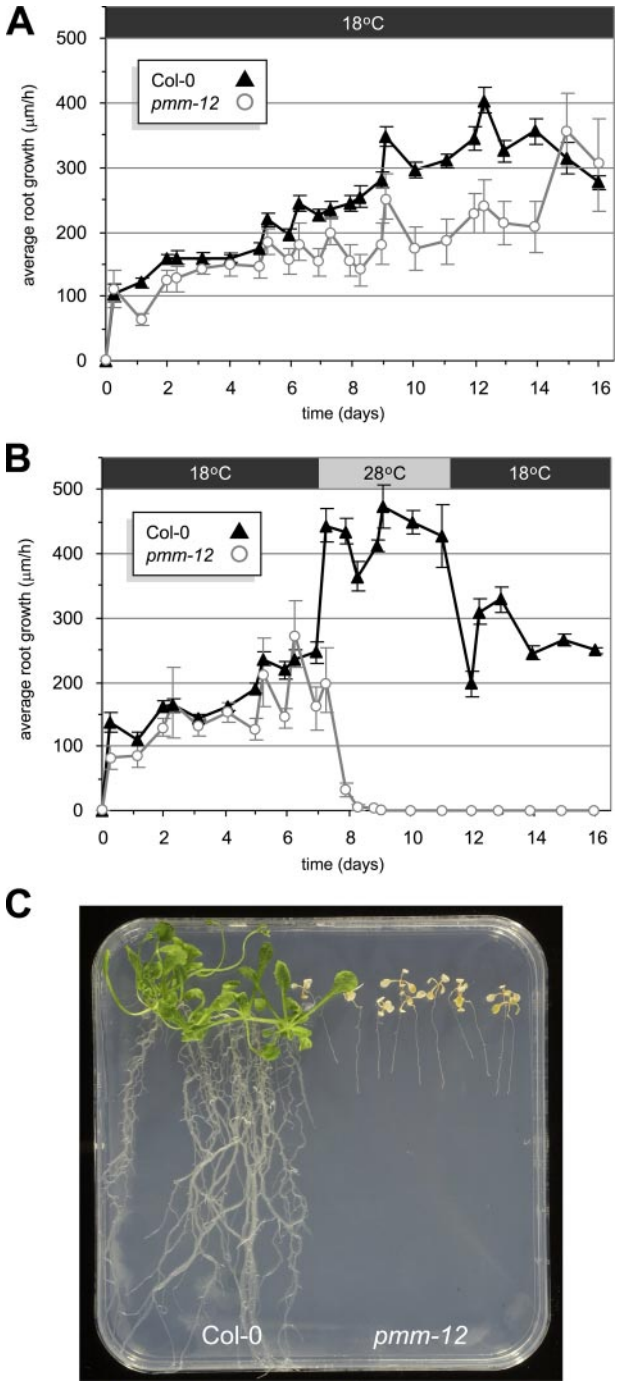

FIGURE 5. **Inhibition of *pmm-12* root growth upon transfer to restrictive temperature.** Primary root growth rates (in μm/h) of Col-0 wild type and *pmm-12* mutant plants grown for 16 days at 18 °C (*A*) or for 7 days at 18 °C, 4 days at 28 °C, and finally placed back to 18 °C for 5 days (*B*). Each data point was calculated by dividing the average root length difference by the time. S.E. values are indicated (n = 8–14). *C*, typical plate with 7-day-old Col-0 wild type and *pmm-12* mutant seedlings (grown at 18 °C), 4 days after transfer to 28 °C.

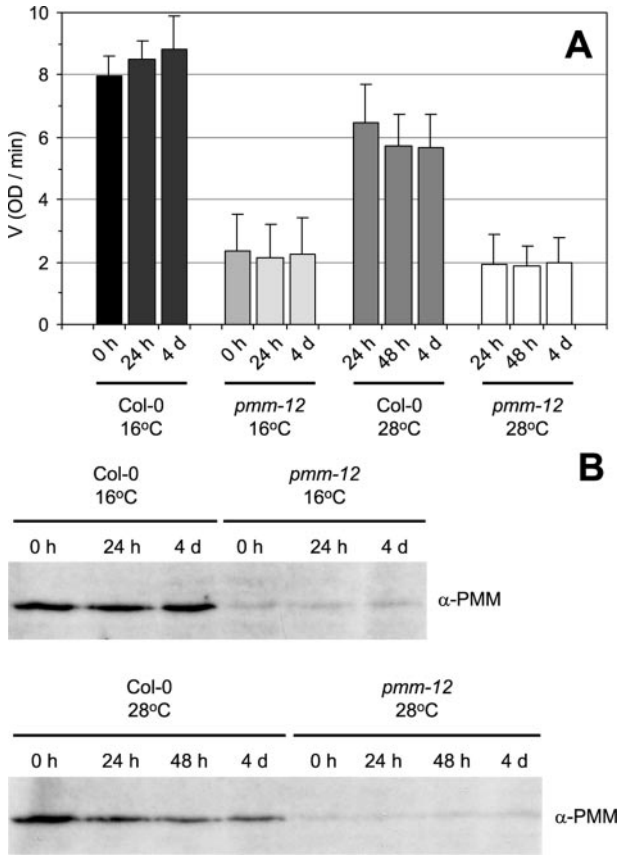

FIGURE 6. **Reduction of PMM enzyme activity and protein levels in *pmm-12* plants.** *A*, PMM activity of total protein extracts isolated from both wild type (Col-0) and *pmm-12* mutant seedlings, initially grown at 16 °C for 2 weeks and subsequently transferred to 28 °C for 24 h, 48 h, or 4 days. Proteins were isolated from at least 40 pooled seedlings, and equal amounts of total protein were used for each sample. As a substrate, 1 mM D-mannose 1-phosphate was used. Values are averages of three measurements. *B*, Western blot of protein extracts used in enzyme activity measurements probed with polyclonal *Arabidopsis* PMM antibody (α-PMM) detecting a protein of ~30 kDa. Equal amounts of protein (25 μg) were loaded in each *lane*. *Error bars* depict S.E.

containing both point mutations (PMM-12). Kinetic parameters of the His-tagged purified proteins were determined at both 18 and 28 °C. The different PMM isoforms displayed distinct kinetic properties. At 18 °C, the turnover numbers (K_{cat}) of wild type PMM and PMM-1 were nearly identical, whereas those of both PMM-2 and PMM-12 were markedly reduced, with K_{cat} values of 11 and 4% relative to wild type values, respectively. The K_m value of wild type PMM was 387 ± 28 μM, comparable with that of PMM-1 (475 ± 34 μM). Unexpectedly, the K_m of PMM-12 was roughly 2-fold lower. Nevertheless, the stacked mutations resulted in a catalytic efficiency (K_{cat}/K_m) that was only 8% of the wild type value. No differential effects of assay temperature on K_{cat}/K_m were observed (Table 1). Taken together, these data indicate that the decrease in catalytic activity of the mutant PMM-12 enzyme is largely due to the *pmm-2* mutation. Second, the strong decrease in catalytic efficiency of PMM-12 observed at 28 °C is comparable with that at 18 °C.

The pmm-12 Cell Death Phenotype Is Not Caused by AsA Deficiency—Reduction of PMM expression levels through virus-induced gene silencing in *N. benthamiana* has been shown to result in decreased AsA levels (3). Therefore, we measured AsA levels in *pmm-12* after transfer to restrictive temperature, using the ascorbate-deficient *vtc1* mutant (11, 12) as a reference. In wild type plants, AsA levels increased significantly after transfer to 28 °C, whereas in *pmm-12* plants they remained relatively stable and amounted to only 20–50% of wild type levels. In fact, AsA content in *pmm-12* seedlings was very comparable with that in *vtc1*, either when expressed per g

TABLE 1

Kinetic properties of purified recombinant wild type (PMM-WT) and mutant (PMM-1, PMM-2, or PMM-12) *Arabidopsis* PMM proteins, determined at 18 and 28 °C

Enzymes were assayed by monitoring NADPH formation in a coupled assay. The indicated values are averages ± S.D. ($n = 3$).

	K_m		K_{cat}		K_{cat}/K_m	
	18 °C	28 °C	18 °C	28 °C	18 °C	28 °C
	μM		s^{-1}		$s^{-1}\,M^{-1}$	
PMM-WT	387 ± 28	200 ± 15	4.13 ± 0.11	10.01 ± 0.23	10.7×10^3	50.1×10^3
PMM-1 (G7R)	475 ± 34	229 ± 18	4.18 ± 0.11	10.31 ± 0.25	8.8×10^3	45.1×10^3
PMM-2 (R37Q)	294 ± 21	111 ± 8	0.44 ± 0.01	0.67 ± 0.01	1.5×10^3	6.0×10^3
PMM-12 (G7R/R37Q)	204 ± 13	68 ± 5	0.18 ± 0.00	0.24 ± 0.00	0.9×10^3	3.7×10^3

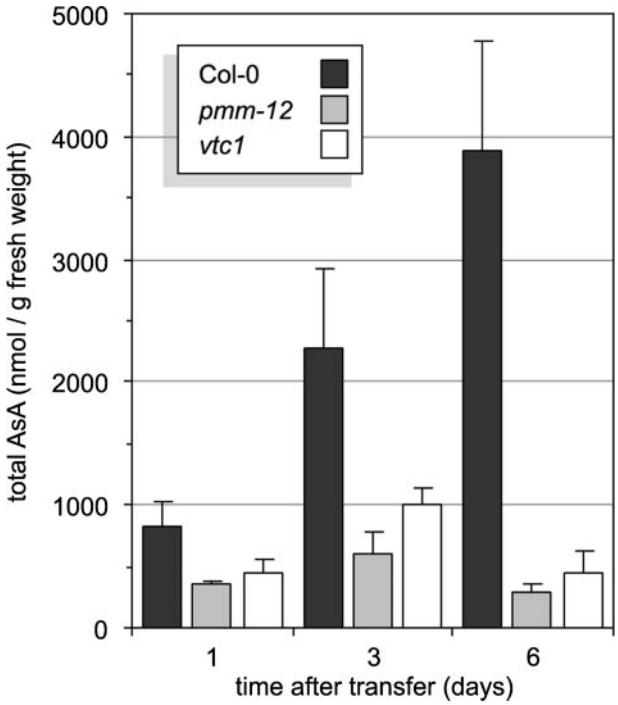

FIGURE 7. **Leaf AsA content per g fresh weight of 2-week-old wild type (Col-0), *pmm-12*, and *vtc1* seedlings grown at 16 °C, after transfer to 28 °C.** AsA levels were calculated from three independent observations. *Error bars*, S.E.

fresh weight (Fig. 7) or per g of chlorophyll (data not shown). However, despite their relatively low AsA content, *vtc1* seedlings showed neither enhanced growth retardation nor cell death following transfer to 28 °C. In addition, we tried to complement the ts phenotype of *pmm-12* with L-galactono-1,4-lactone, the immediate precursor of AsA. Although AsA levels increased in *pmm-12* seedlings grown on MS medium supplemented with 6 mM L-galactono-1,4-lactone, cell death could not be prevented after transfer to 28 °C (data not shown). Taken together, these results indicate that the cell death phenotype observed in *pmm-12* plants is not caused by AsA deficiency.

Protein Glycosylation in the pmm-12 Mutant is Temperature-sensitive—GDP-mannose is required for the synthesis of the core glycan chain that is attached to *N*-linked glycoproteins (5). Therefore, we studied the effect of the temperature shift on total glycoproteins by affinodetection with ConA, a lectin that binds to the terminal mannose residue of *N*-linked oligosaccharides (30). Several differences in protein composition were observed in extracts from *pmm-12* mutant plants transferred to 28 °C compared with extracts from plants kept at

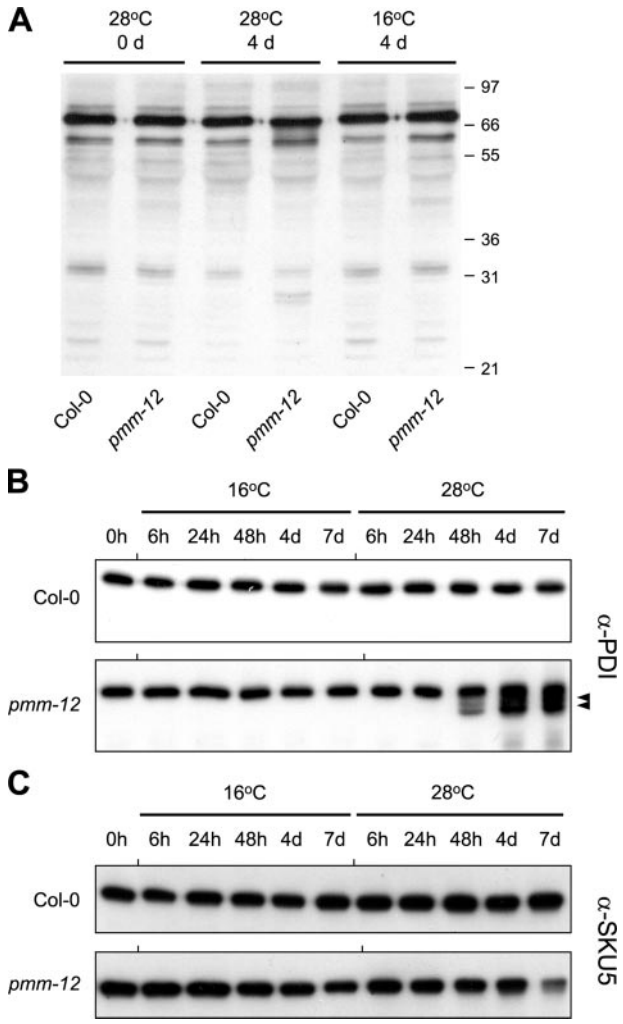

FIGURE 8. **Effect of the *pmm-12* mutation on protein glycosylation and GPI anchoring.** Protein was extracted from both wild type (Col-0) and mutant seedlings, initially grown at 16 °C for 2 weeks and subsequently transferred to 28 °C for 6 h, 24 h, 48 h, 4 days, or 7 days. *A*, affinodetection of glycoproteins containing high mannose type *N*-glycans with ConA. Protein sizes (in kDa) are indicated on the *right*. *B*, *N*-glycosylation of PDI, visualized via protein gel blotting, in *pmm-12* plants is affected by transfer to restrictive temperature. The *arrows* on the *right* point out the electrophoretic migration of the mono- and nonglycosylated forms of PDI, in contrast to the upper band corresponding to the fully (di)glycosylated protein. *C*, protein gel blot detection of SKU5 in wild type and *pmm-12* plants after transfer to restrictive temperature.

16 °C or wild type plants. For example, there was a small but marked shift in the position of some bands at about 66-kDa protein, which moved to a lower molecular mass. Moreover, two new bands of ~30 kDa were detected following transfer to 28 °C (Fig. 8*A*).

A defect in *N*-glycosylation has been shown to result in the perturbed addition of *N*-glycans to PDI, a phenomenon that can be detected as a band shift on a protein gel blot (24, 31). PDI is an abundant protein of the endoplasmic reticulum that is posttranslationally modified with *N*-linked glucans (32, 33). We therefore analyzed the effect of the temperature shift on the mobility of PDI extracted from wild type and *pmm-12* seedlings by using specific antibodies. PDI obtained from wild type seedlings, initially grown at 16 °C and subsequently transferred to 28 °C, had a stable molecular mass of ~62 kDa (Fig. 8*B*). However, with PDI obtained from *pmm-12* mutant seedlings, two bands of lower molecular mass appeared 48 h after transfer to 28 °C (Fig. 8*B*). On overexposed films, these bands were detectable 24 h after transfer to 28 °C (data not shown). Note that the cell death phenotype only became apparent 4 days after the temperature shift (Fig. 4).

Another posttranslational protein modification depending on GDP-mannose is the addition of a GPI membrane anchor (34). We used antibodies to *Arabidopsis* SKU5, a protein that has been shown to be degraded in the absence of a functional GPI anchor (35), to investigate whether in *pmm-12* the temperature shift might also trigger a defect in GPI anchoring. SKU5 protein levels were decreased in mutant plants, 7 days after transfer to 28 °C (Fig. 8*C*) and 3 days after the appearance of the cell death phenotype (compare with Fig. 4*B*).

DISCUSSION

Map-based Cloning of the pmm-12 Mutation Locus—During a genetic screen, aimed at identifying EMS-induced ts mutations in *Arabidopsis* genes involved in growth and development, we isolated a ts mutant that died within several days upon transfer to restrictive temperature. The mutation was initially mapped to a 673-kb region on the lower arm of chromosome II by scoring a limited set of physically mapped AFLP markers segregating in 310 F_2 individuals. AFLP markers segregating in the F_2 population were co-dominantly scored (see "Experimental Procedures"). Co-dominant scoring of AFLP markers makes it possible to unequivocally distinguish homozygous from heterozygous plants based on quantitative measurements of the band intensities. This strategy allows the extraction of additional genetic information from the AFLP fingerprints resulting in a more precise delineation of the region of interest. Further fine mapping eventually revealed that the affected gene (at2g45790) encoded a PMM and, remarkably, that there were two point mutations present in the DNA sequence of the gene cloned from the *pmm-12* mutant compared with the wild type gene present in the public data base.

The Temperature-sensitive pmm-12 Mutant Offers a Unique Tool for Functional Characterization of Plant PMM—Based on sequence similarity, the *Arabidopsis* genome contains a single *PMM* gene (at2g45790). During the preparation of this manuscript, it was reported that the encoded protein indeed showed PMM activity, effectively converting mannose 1-phosphate to mannose 6-phosphate (3). Overexpression and virus-induced gene silencing knockdown experiments in *Arabidopsis* and *N. benthamiana*, respectively, indicated a role for PMM in AsA biosynthesis. However, no *pmm* knock-out mutants were reported, and efforts to obtain knockdown lines via RNA interference were unsuccessful. The lack of such mutants impaired assessment of the possible involvement of PMM in processes other than AsA biosynthesis (3). Thus, the conditional phenotype of the ts *pmm-12* mutant described here has enabled us to further characterize PMM functions in plants. The data presented show that the ts *pmm-12* mutant is a unique tool with which to study the molecular function of the *Arabidopsis PMM* gene and to characterize the role of PMM and GDP-mannose in plant growth and development.

PMM Enzyme Activity Is Differentially Affected by the pmm-1 and pmm-2 Mutations—PMMs are members of the magnesium-dependent phosphotransferase superfamily of haloalkanoic acid dehalogenases that catalyze phosphoryl group transfer reactions (27). All members of the haloalkanoic acid dehalogenase superfamily, including PMMs, possess a tertiary structure consisting of a typical α/β core domain and a second cap domain, with the active site located at the domain-domain interface. Transfer of the phosphoryl group is mediated by a strongly conserved aspartate nucleophile in the core domain (28) that has a highly conserved tertiary structure, whereas the cap domain that determines substrate specificity is more divergent in sequence and length (36, 37). Both the *pmm-1* and *pmm-2* mutations are located in the core domain. However, by using the PSIRED tool (38), the GenTHREADER tool (39), and the crystal structure of human PMM1 as a template (37), we inferred that the affected amino acid residues are most probably not essential for catalysis or substrate binding (data not shown). Nevertheless, the identified point mutations might disrupt the highly conserved tertiary structure of the core domain, because both amino acid substitutions are rather drastic. The *pmm-1* mutation changes a neutral aliphatic glycine residue into a positively charged basic arginine, whereas *pmm-2* results in the substitution of an arginine into a negatively charged acidic glutamine. In addition, the arginine affected by *pmm-2* is highly conserved among virtually all PMMs present in public data bases (data not shown), suggesting that it is important for adequate functioning of the protein.

In vitro assays with the different recombinant mutant PMM isoforms (performed at both 18 and 28 °C) showed that the *pmm-2* mutation resulted in a significant reduction in PMM enzyme activity, whereas the *pmm-1* mutation only marginally affected enzyme kinetics (Table 1). This result implies that, due to the location and/or nature of the amino acid substitution, the *pmm-1* mutation alone would have few biological consequences. The activity assays also revealed that the observed decrease in catalytic efficiency of PMM-12 is independent of the assay temperature. When viewed together with the observed decreases in PMM protein and enzyme activity observed at 18 °C (Fig. 6), these results indicate that the *pmm-12* mutant is not a typical ts mutant in the sense that the protein becomes inactive or unstable only at restrictive temperature. Rather, the data suggest that *Arabidopsis* plants growing at 18 °C can cope with reduced PMM enzymatic capacity, whereas in plants growing at 28 °C this becomes lethal.

Aberrant Protein Glycosylation Precedes the Cell Death Phenotype—Disturbed PMM enzyme activity will probably lead to GDP-mannose deficiency and have pleiotropic effects. PMM has been described to play an important role in the biosynthesis

of AsA (2, 3). Therefore, we first tested whether *pmm-12* contained less AsA than wild type plants. Our measurements indicated that, after transfer to restrictive temperature, AsA levels in the *pmm-12* mutant were only 20–50% of those in wild type plants and comparable with those in the AsA mutant *vtc1* (Fig. 7). This result strengthens the genetic evidence for PMM involvement in AsA biosynthesis. During this experiment, it was noted that *vtc1*, unlike *pmm-12*, did not display cell death when transferred to 28 °C. Moreover, supplying the *pmm-12* mutant with the immediate precursor of AsA, L-galactono-1,4-lactone, did not prevent the occurrence of cell death after transfer to 28 °C (data not shown). Taken together, these results demonstrate that the ts cell death phenotype observed in the *pmm* mutant is not caused by AsA deficiency.

Besides its role in AsA biosynthesis, GDP-mannose also plays a key role in posttranslational modifications, such as protein glycosylation. *N*-Glycosylation is essential for proper folding, targeting, and function of many secreted proteins. The core glycan attached to *N*-linked glycoproteins is assembled on a dolichol phosphate and contains nine mannose residues, which are transferred to it from GDP-mannose (4). The results presented here indicate that, shortly after the temperature shift, a deficiency in *N*-glycosylation occurs in *pmm-12* plants. In addition, GPI anchoring, a second posttranslational protein modification depending on GDP-mannose (34), is affected several days later (Fig. 8). Based on these observations, we propose that the cell death phenotype of *pmm-12* plants at restrictive temperature and the embryo lethality observed in the T-DNA insertion knock-out line are caused by strongly decreased PMM activity, eventually leading to a deficiency in *N*-glycosylation.

Various examples in the literature support the hypothesis that glycosylation defects can result in cell death and lethality. In both yeast and animals, aberrations in protein glycosylation have been linked to cell death. Mutations that block early steps in the assembly of core glycans (*e.g. alg1*, *alg2*, *alg4*, and *vig9*) are lethal (40, 41) as is the knock-out mutation of the yeast *PMM* gene *SEC53* (6). Furthermore, glycosylation mutants with defects in the oligosaccharyltransferase protein complex were reported to undergo programmed cell death (42, 43). In *Arabidopsis*, mutant alleles of the gene encoding GCS1/KNF, a protein necessary for complex *N*-glycan formation, and the genes encoding DGL1 and STT3, two different subunits of the *Arabidopsis* oligosaccharyltransferase complex, have been described to result in aborted embryos or to produce nonviable seeds (31, 44–46).

The *Arabidopsis cyt1* mutation abolishes GMPP gene function and results in embryo lethality by arresting embryonic development at a very early stage, providing strong evidence for the lethality of a severe GMPP deficiency. Characteristic aspects of the *cyt1* phenotype can be mimicked with tunicamycin, an inhibitor of *N*-glycosylation. This observation led to the conclusion that a deficiency in this process can account for most of the phenotypic features of *cyt1* (24). It is interesting to note that GMPP acts directly downstream of PMM in the GDP-mannose biosynthesis pathway (Fig. 1). However, similar to the *pmm-12* mutant, *cyt1* could not be rescued by exogenously applied AsA (24), suggesting that in both cases the lack of AsA is not sufficient to explain the developmental arrest and subsequent cell death. The *cyt1* mutant is allelic to *vtc1*, a mutant deficient in its AsA biosynthesis (12) that was isolated by virtue of its sensitivity to oxidative stress (47). In marked contrast to the lethality caused by *cyt1* mutations, *vtc1* plants are viable and fertile, indicating that the *vtc1* mutation is weak. Consistently, GMPP activity is reduced but not absent from *vtc1* protein extracts (11).

The evidence described above demonstrates that the lethality of the *pmm-12* mutation results from glycosylation defects rather than AsA depletion. It remains intriguing why the GDP-mannose depletion in *pmm-12* is severe enough to result in cell death, whereas its AsA levels remain comparable to those in *vtc1*. The presence of alternative biosynthesis or recycling pathways for AsA that are independent of mannose would provide an explanation for this paradox (48). However, a recent analysis of the *vtc2 vtc5* double mutants has revealed that the GDP-mannose pathway is the only significant source of AsA in *Arabidopsis* seedlings (49). Another potential explanation would be that *pmm-12* prioritizes the flux through GDP-mannose toward AsA biosynthesis at the expense of glycosylation. More detailed comparisons of the regulation of AsA synthesis in the *vtc* mutants and *pmm-12* are required in order to determine whether any form of prioritization exists *in planta*. Although this comparison is beyond the scope of the present paper, it is possible to consider factors that might influence the path of metabolite flow, such as toxic effects of elevated mannose 6-phosphate or a role for mannose 1-phosphate in cell survival.

Acknowledgments—We thank Michaël Vandorpe, Misha de Beer, and Wilson Ardiles Diaz for excellent technical assistance; Dr. Nico Callewaert, Dr. Pierre Lejeune, and Dr. Annie Jacqmard for helpful discussions; and Dr. Martine De Cock for help with preparing the manuscript. We also kindly thank Dr. Chris R. Somerville for the PDI antibody and Dr. John C. Sedbrook for the SKU5 antibody.

REFERENCES

1. Seifert, G. J. (2004) *Curr. Opin. Plant Biol.* **7,** 277–284
2. Wheeler, G. L., Jones, M. A., and Smirnoff, N. (1998) *Nature* **393,** 365–369
3. Qian, W., Yu, C., Qin, H., Liu, X., Zhang, A., Johansen, I. E., and Wang, D. (2007) *Plant J.* **49,** 399–413
4. Lerouge, P., Cabanes-Macheteau, M., Rayon, C., Fischette-Lainé, A.-C., Gomord, V., and Faye, L. (1998) *Plant Mol. Biol.* **38,** 31–48
5. Spiro, R. G. (2002) *Glycobiology* **12,** 43R–56R
6. Bernstein, M., Hoffmann, W., Ammerer, G., and Schekman, R. (1985) *J. Cell Biol.* **101,** 2374–2382
7. Kepes, F., and Schekman, R. (1988) *J. Biol. Chem.* **263,** 9155–9161
8. Garami, A., Mehlert, A., and Ilg, T. (2001) *Mol. Cell. Biol.* **21,** 8168–8183
9. Thiel, C., Lübke, T., Matthijs, G., von Figura, K., and Körner, C. (2006) *Mol. Cell. Biol.* **26,** 5615–5620
10. Van Schaftingen, E., and Jaeken, J. (1995) *FEBS Lett.* **377,** 318–320
11. Conklin, P. L., Norris, S. R., Wheeler, G. L., Williams, E. H., Smirnoff, N., and Last, R. L. (1999) *Proc. Natl. Acad. Sci. U. S. A.* **96,** 4198–4203
12. Conklin, P. L., Pallanca, J. E., Last, R. L., and Smirnoff, N. (1997) *Plant Physiol.* **115,** 1277–1285
13. Karimi, M., Inzé, D., and Depicker, A. (2002) *Trends Plant Sci.* **7,** 193–195
14. Clough, S. J., and Bent, A. F. (1998) *Plant J.* **16,** 735–743
15. Peters, J. L., Cnops, G., Neyt, P., Zethof, J., Cornelis, K., Van Lijsebettens, M., and Gerats, T. (2004) *Theor. Appl. Genet.* **108,** 321–327
16. Peters, J. L., Constandt, H., Neyt, P., Cnops, G., Zethof, J., Zabeau, M., and Gerats, T. (2001) *Plant Physiol.* **127,** 1579–1589

17. Vuylsteke, M., Peleman, J. D., and van Eijk, M. J. T. (2007) *Nat. Protocols* **2,** 1387–1398
18. Jander, G., Norris, S. R., Rounsley, S. D., Bush, D. F., Levin, I. M., and Last, R. L. (2002) *Plant Physiol.* **129,** 440–450
19. Rozen, S., and Skaletsky, H. (2000) *Methods Mol. Biol.* **132,** 365–386
20. Bradford, M. M. (1976) *Anal. Biochem.* **72,** 248–254
21. Hancock, R. D., McRae, D., Haupt, S., and Viola, R. (2003) *BMC Plant Biol.* **3,** 7.1–7.13
22. Vernon, L. P. (1960) *Anal. Chem.* **32,** 1144–1150
23. Foyer, C., Rowell, J., and Walker, D. (1983) *Planta* **157,** 239–244
24. Lukowitz, W., Nickle, T. C., Meinke, D. W., Last, R. L., Conklin, P. L., and Somerville, C. R. (2001) *Proc. Natl. Acad. Sci. U. S. A.* **98,** 2262–2267
25. Vaeck, E. (2006) Ph.D. thesis, Ghent University, Gent, Belgium
26. Bell, C. J., and Ecker, J. R. (1994) *Genomics* **19,** 137–144
27. Koonin, E. V., and Tatusov, R. L. (1994) *J. Mol. Biol.* **244,** 125–132
28. Collet, J.-F., Stroobant, V., Pirard, M., Delpierre, G., and Van Schaftingen, E. (1998) *J. Biol. Chem.* **273,** 14107–14112
29. Rosso, M. G., Li, Y., Strizhov, N., Reiss, B., Dekker, K., and Weisshaar, B. (2003) *Plant Mol. Biol.* **53,** 247–259
30. Faye, L., and Chrispeels, M. J. (1985) *Anal. Biochem.* **149,** 218–224
31. Lerouxel, O., Mouille, G., Andème-Onzighi, C., Bruyant, M.-P., Séveno, M., Loutelier-Bourhis, C., Driouich, A., Höfte, H., and Lerouge, P. (2005) *Plant J.* **42,** 455–468
32. Shorrosh, B. S., Subramaniam, J., Schubert, K. R., and Dixon, R. A. (1993) *Plant Physiol.* **103,** 719–726
33. Shimoni, Y., Zhu, X.-z., Levanony, H., Segal, G., and Galili, G. (1995) *Plant Physiol.* **108,** 327–335
34. Kinoshita, T., and Inoue, N. (2000) *Curr. Opin. Chem. Biol.* **4,** 632–638
35. Gillmor, C. S., Lukowitz, W., Brininstool, G., Sedbrook, J. C., Hamann, T., Poindexter, P., and Somerville, C. (2005) *Plant Cell* **17,** 1128–1140
36. Morais, M. C., Zhang, W., Baker, A. S., Zhang, G., Dunaway-Mariano, D., and Allen, K. N. (2000) *Biochemistry* **39,** 10385–10396
37. Silvaggi, N. R., Zhang, C., Lu, Z., Dai, J., Dunaway-Mariano, D., and Allen, K. N. (2006) *J. Biol. Chem.* **281,** 14918–14926
38. Jones, D. T. (1999) *J. Mol. Biol.* **292,** 195–202
39. McGuffin, L. J., and Jones, D. T. (2003) *Bioinformatics* **19,** 874–881
40. Hashimoto, H., Sakakibara, A., Yamasaki, M., and Yoda, K. (1997) *J. Biol. Chem.* **272,** 16308–16314
41. Kukuruzinska, M. A., and Lennon-Hopkins, K. (1999) *Biochim. Biophys. Acta* **1426,** 359–372
42. Nakashima, T., Sekiguchi, T., Kuraoka, A., Fukushima, K., Shibata, Y., Komiyama, S., and Nishimoto, T. (1993) *Mol. Cell. Biol.* **13,** 6367–6374
43. Silberstein, S., Collins, P. G., Kelleher, D. J., and Gilmore, R. (1995) *J. Cell Biol.* **131,** 371–383
44. Boisson, M., Gomord, V., Audran, C., Berger, N., Dubreucq, B., Granier, F., Lerouge, P., Faye, L., Caboche, M., and Lepiniec, L. (2001) *EMBO J.* **20,** 1010–1019
45. Gillmor, C. S., Poindexter, P., Lorieau, J., Palcic, M. M., and Somerville, C. (2002) *J. Cell Biol.* **156,** 1003–1013
46. Koiwa, H., Li, F., McCully, M. G., Mendoza, I., Koizumi, N., Manabe, Y., Nakagawa, Y., Zhu, J., Rus, A., Pardo, J. M., Bressan, R. A., and Hasegawa, P. M. (2003) *Plant Cell* **15,** 2273–2284
47. Conklin, P. L., Williams, E. H., and Last, R. L. (1996) *Proc. Natl. Acad. Sci. U. S. A.* **93,** 9970–9974
48. Wolucka, B. A., and Van Montagu, M. (2007) *Phytochemistry* **68,** 2602–2613
49. Dowdle, J., Ishikawa, T., Gatzek, S., Rolinski, S., and Smirnoff, N. (2007) *Plant J.* **52,** 673–689